

Controls on and effects of armoring and vertical sorting in aeolian dune fields: A numerical simulation study

Xin Gao, Clément Narteau, Olivier Rozier

▶ **To cite this version:**

Xin Gao, Clément Narteau, Olivier Rozier. Controls on and effects of armoring and vertical sorting in aeolian dune fields: A numerical simulation study. Geophysical Research Letters, 2016, 43, pp.2614-2622. 10.1002/2016GL068416 . insu-03581672

HAL Id: insu-03581672

https://insu.hal.science/insu-03581672

Submitted on 20 Feb 2022

HAL is a multi-disciplinary open access archive for the deposit and dissemination of scientific research documents, whether they are published or not. The documents may come from teaching and research institutions in France or abroad, or from public or private research centers.

L'archive ouverte pluridisciplinaire **HAL**, est destinée au dépôt et à la diffusion de documents scientifiques de niveau recherche, publiés ou non, émanant des établissements d'enseignement et de recherche français ou étrangers, des laboratoires publics ou privés.

Copyright

AGU PUBLICATIONS

Geophysical Research Letters

RESEARCH LETTER
10.1002/2016GL068416

Key Points:
- Grain size vertical sorting occurs during dune growth
- The development of an armor layer controls sediment availability
- The emergence of dunes and the subsequent dune types depend on the grain size distribution

Supporting Information:
- Supporting Information S1

Correspondence to:
X. Gao,
gao@ipgp.fr

Citation:
Gao, X., C. Narteau, and O. Rozier (2016), Controls on and effects of armoring and vertical sorting in aeolian dune fields: A numerical simulation study, *Geophys. Res. Lett.*, *43*, 2614–2622, doi:10.1002/2016GL068416.

Received 24 FEB 2016
Accepted 26 FEB 2016
Accepted article online 29 FEB 2016
Published online 23 MAR 2016

©2016. American Geophysical Union. All Rights Reserved.

Controls on and effects of armoring and vertical sorting in aeolian dune fields: A numerical simulation study

Xin Gao[1], Clément Narteau[1], and Olivier Rozier[1]

[1] Institut de Physique du Globe de Paris, Sorbonne Paris Cité, Université Paris Diderot, Paris, France

Abstract Unlike ripples, there are only few numerical studies on grain size segregation at the scale of dunes in aeolian environments. Here we use a cellular automaton model to analyze vertical sorting in granular mixtures under steady unidirectional flow conditions. We investigate the feedbacks between dune growth and the segregation mechanisms by varying the size of coarse grains and their proportion within the bed. We systematically observe the development of a horizontal layer of coarse grains at the top of which sorted bed forms may grow by amalgamation. The formation of such an armor layer controls the overall sediment transport and availability. The emergence of dunes and the transition from barchan to transverse dune fields depend only on the grain size distribution of the initial sediment layer. As confirmed by observation, this result indicates that armor layers should be present in most arid deserts, where they are likely to control dune morphodynamics.

1. Introduction

Sediment availability controls bed forms, especially in aeolian settings where wind directional variability must also be considered as a primary factor for dune shape [*Wasson and Hyde*, 1983; *Courrech du Pont et al.*, 2014]. However, sediment availability remains poorly defined and somewhat controversial in most natural environments. This is mainly due to the wide range of grain sizes, which introduces different levels of complexity in the sediment transport process [*Lancaster*, 1986; *Dong et al.*, 2008; *Frey and Church*, 2009]. In this case, the development of coarse-grained surfaces by selective transport is a particularly important issue, which has been widely examined in various subaqueous systems [*Parker and Klingeman*, 1982; *Dietrich et al.*, 1989; *Blom et al.*, 2003; *Murray and Thieler*, 2004; *Coco et al.*, 2007a] but never addressed as a formative process in arid sand seas. Here we study the development of dunes in granular mixtures incorporating two grain size populations in a cellular automaton dune model. We work at the intermediate length scale of the sand flux saturation [*Andreotti et al.*, 2010], at which we aggregate the effects of the smaller-scale processes on transport (i.e., individual grain motions and saltation). Thus, we can study larger systems and concentrate on the interactions between dune morphodynamics (Figure 1) and the mechanisms of size segregation (selective transport and avalanching).

When avalanching takes place in granular mixtures, vertical grain size sorting occurs systematically by kinematic sieving: smaller grains tend to penetrate and migrate downward, while larger ones tend to rise to the top. Entirely controlled by the contact dynamics and solid friction at grain-grain interfaces [*Staron and Phillips*, 2014], this interparticle percolation creates a layer of fine material on the top of which larger grains can roll more easily without being captured. As a consequence, coarse grains propagate over longer distances to form their own deposits at the base of sand piles. Ultimately, the repetition of individual avalanches can also produce stratified layers of coarse and fine sediment [*Makse et al.*, 1997; *Cizeau et al.*, 1999].

In the presence of shear flow, another major source of size segregation is associated with the entrainment of grains by fluid drag and lift forces. These forces have to balance gravity in order to set grains into motion. Hence, there is a threshold shear stress for motion inception, which may change not only with respect to grain size but also according to the configuration of the bed [*Houssais and Lajeunesse*, 2012]. For example, the concept of equal mobility suggests that the bed surface texture evolves to a state in which all grains, whatever their size, have the same threshold entrainment stress [*Parker and Klingeman*, 1982]. However, larger grains are intrinsically less likely to be entrained by the flow than smaller ones. Considering fractional transport rates,

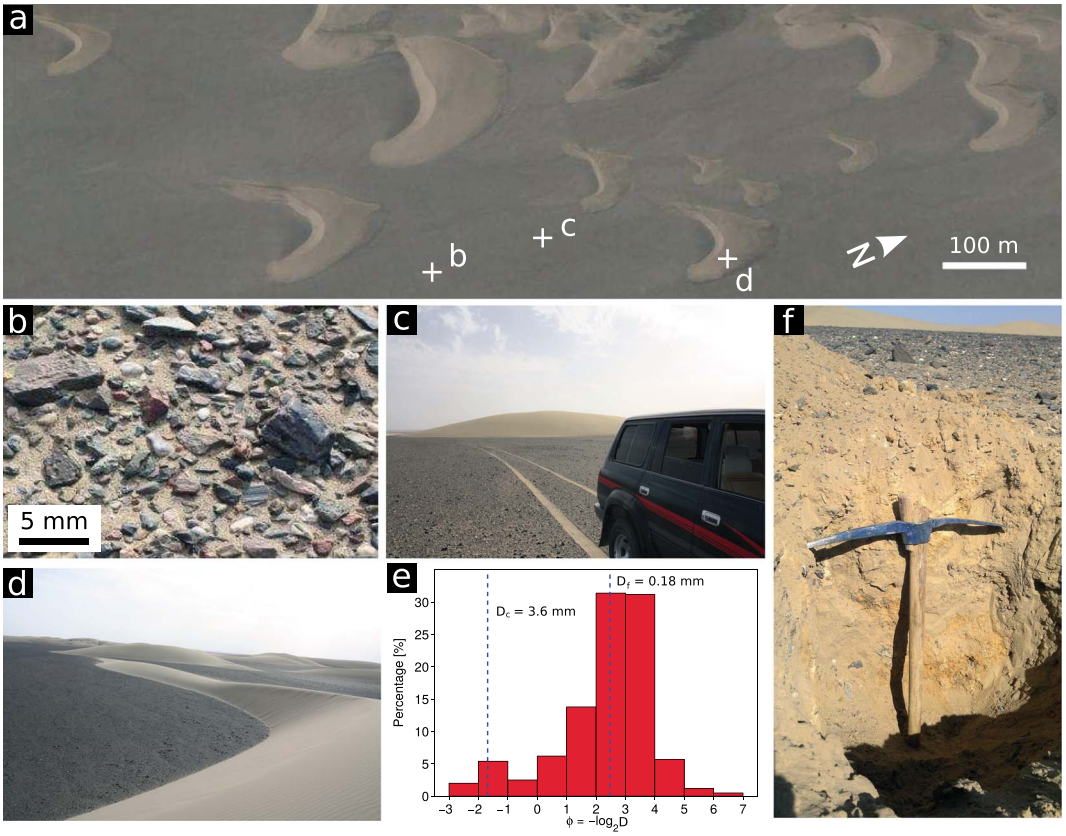


Figure 1. Dunes, armoring, and vertical sorting in the Kumtagh Desert (China, 40°36′ N, 92°57′E). (a) Barchan dune field. (b) The armor layer composed of coarse grains. (c) Surface and subsurface sediment layers. (d) View of the barchan dune field from a dune crest. (e) Grain size distribution 10 cm below the surface layer. Coarse clasts larger than 8 mm ($\phi < -3$) have not been weighted. (f) The original alluvial deposits where the grain size has been measured. Positions where Figures 1b–1d have been taken are reported in Figure 1a. The barchan dunes and the subsurface layer are essentially composed of fine material. The pavement protects the subsurface sediment layer from wind erosion. Coarse grains are darker because they contain less quartz and more andesite and dacite than finer grains [*Dong et al.*, 2008]. Below the surface layer, the well-mixed sediment layer exhibits a bimodal grain size distribution with two peaks at 180 μm and 3.6 mm. The fine end-member of the subsurface has the same size distribution as the dunes.

smaller grains contribute more to transport than coarser ones [*Wilcock and Southard*, 1989], such that the winnowing of fine particles may locally affect the grain size distribution (Figure 1b). Where the proportion of coarse grains increases, it may generate an armor layer wherein larger particles may become essentially immobile (Figure 1c). Such a formation of a pavement by selective transport stabilizes the bed and limits the vertical exchanges of material [*Dietrich et al.*, 1989]. In addition, it offers a rougher surface on the top of which patches of fine grains may appear, propagate, and grow in size by amalgamation (Figures 1a and 1d).

As soon as dunes develop, changes in topography locally modify the bed shear stress and sediment transport rates. Steeper slopes result in gravity-driven granular flows, which may in turn amplify vertical grain size sorting. Furthermore, migrating dunes have an impact on sand availability as they control the exposure of the underlying sediment layer to the flow (Figures 1a and 1d). These feedbacks between the topography and the variation of the bed composition over depth involve a variety of interactions which remain difficult to incorporate into continuous sediment transport models [*Parker et al.*, 2000]. Then, a large number of studies have examined sediment sorting in rivers, the inner continental shelf and aeolian ripples through field observations, laboratory experiments, and numerical methods [*Anderson and Bunas*, 1993; *Wilcock*, 2001; *Blom et al.*, 2003; *Murray and Thieler*, 2004; *Blom et al.*, 2008]. In comparison, there are only a few, limited studies on the development of aeolian dune patterns from granular mixtures [*Thomas*, 2011]. Our study contributes to this effort by investigating quantitatively how sand availability and dune shape may be related to the original composition of the bed. Simultaneously, we try to give a comprehensive understanding of vertical size segregation during dune growth.

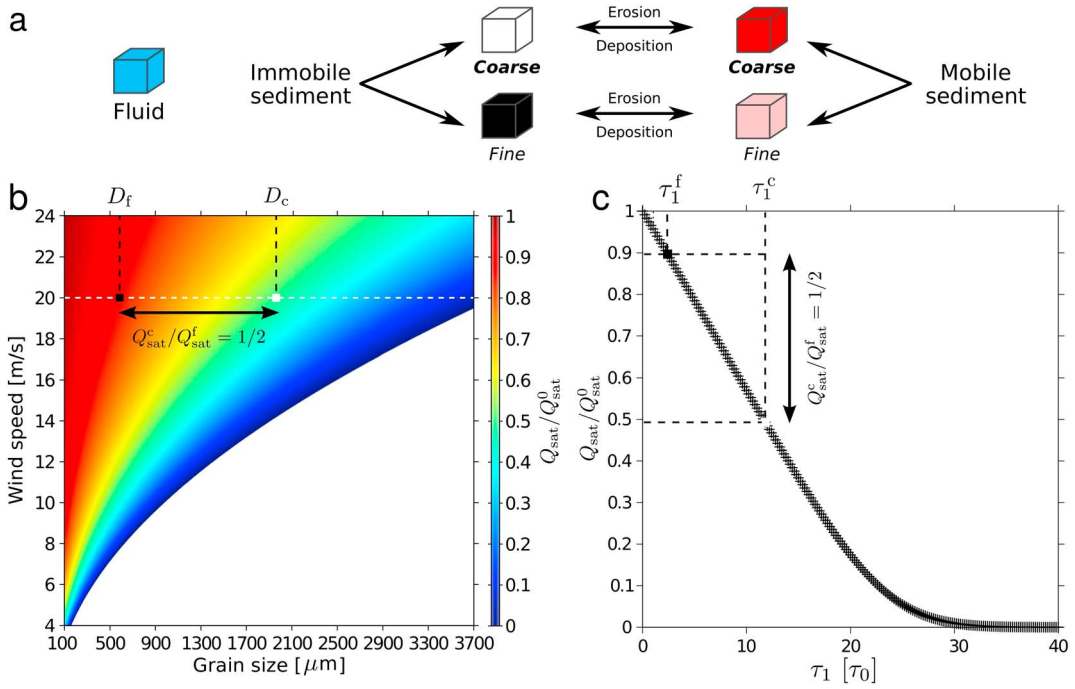


Figure 2. Two grain sizes in the real-space cellular automaton dune model. (a) Sedimentary states are decomposed into substates according to grain size. (b) Normalized saturated flux Q_{sat}/Q^0_{sat} versus grain size and wind speed using Equations (4) to (6) with a parameterization for aeolian dunes on Earth (see Table S1 in the supporting information). The white dashed line shows the wind speed used in the numerical simulations. (c) Normalized saturated flux Q_{sat}/Q^0_{sat} in the model with respect to the threshold shear stress τ_1. Using Figures 2b and 2c, one can determine the τ_1 value in the model for any grain size and wind speed in nature. Similarly, as shown in the example, the coarse grain diameter D_c may be derived from wind speed, a fine grain diameter D_f, and a finite saturated sand flux ratio Q^c_{sat}/Q^f_{sat} (i.e., $Q^f_{sat} > Q^c_{sat} > 0$).

2. Two Grain Sizes in a Real-Space Cellular Automaton Dune Model

The real-space cellular automaton dune model combines a cellular automaton for sediment transport with a lattice-gas cellular automaton for high Reynolds-flow simulation [*Narteau et al.*, 2009; *Rozier and Narteau*, 2014]. In the model of sediment transport, individual physical processes are associated with different sets of transitions between nearest-neighbor cells at the elementary length scale l_0 of a cubic lattice. A cell is defined by its state: fluid, mobile, and immobile sediment (Figure 2a). The stochastic dynamics is defined in terms of transition probabilities per unit of time t_0. For example, Λ_e, Λ_c, and Λ_t are the transition rates for erosion, deposition, and transport, respectively. To take into account avalanching, we impose a repose angle θ_c for the granular material. As the triggering of avalanches depends on the local slope θ, the avalanche transition rate is constant for $\theta \geq \theta_c$ and set to zero for $\theta < \theta_c$. Except for dependencies of the repose angle on grain size all the model parameter values are equal to those presented in Table 1 of *Zhang et al.* [2014].

A lattice-gas model is used to simulate the flow and calculate both the wind speed and the bed shear stress τ_s over space and time. We consider that the erosion rate Λ_e is linearly related to the bed shear stress according to

$$\Lambda_e = \begin{cases} 0 & \text{for } \tau_s \leq \tau_1, \\ \Lambda_0 \dfrac{\tau_s - \tau_1}{\tau_2 - \tau_1} & \text{for } \tau_1 \leq \tau_s \leq \tau_2, \\ \Lambda_0 & \text{else,} \end{cases} \quad (1)$$

where Λ_0 is a constant rate, τ_1 is the threshold for motion inception, and τ_2 is a constant parameter to adjust the slope of the linear relationship. For consistency, we always have $\tau_s \ll \tau_2$. By definition, $(\tau_s - \tau_1)$ is the excess

shear stress. To compute the saturated sand flux on a flat sand bed for different τ_1 values, we use the relation suggested by *Gao et al.* [2014],

$$Q_{\mathrm{sat}}(\tau_1) = \frac{\Lambda_t}{\Lambda_c} \int_{-\infty}^{\infty} \Lambda_e(\tau_s; \tau_1) f(\tau_s) \mathrm{d}\tau_s, \tag{2}$$

where $f(\tau_s)$ is the probability density function of τ_s on a flat sand bed.

In the physics of sediment transport, generic transport laws are usually of the form

$$Q_{\mathrm{sat}} = \begin{cases} 0 & \text{if } \tau_s \le \tau_1, \\ \tau_s^{\gamma}(\tau_s - \tau_1) & \text{if } \tau_s \ge \tau_1, \end{cases} \tag{3}$$

where γ is a positive (or null) constant [*Sherman and Li*, 2012]. Introducing the shear velocity $u_* \equiv \tau_s^{1/2}$, we can compute the ratio between the saturated flux Q_{sat} and its value Q_{sat}^0 for $\tau_1 = 0$,

$$\frac{Q_{\mathrm{sat}}}{Q_{\mathrm{sat}}^0} = 1 - \left(\frac{u_c}{u_*}\right)^2, \tag{4}$$

where u_c is the threshold shear velocity for motion inception. In practice, this entrainment threshold can be derived from the flow speed u measured at a height z using

$$u_* = \frac{u\kappa}{\log(z/z_0)}, \tag{5}$$

where z_0 is the characteristic surface roughness and κ the von-Kármán constant. Independently, the threshold shear velocity for motion inception can be determined using

$$u_c = 0.1\sqrt{\frac{\rho_s}{\rho_f} g D}, \tag{6}$$

where D is the grain diameter, g the gravitational acceleration, and ρ_s/ρ_f the grain to fluid density ratio [*Iversen and Rasmussen*, 1999]. For a given flow speed and a uniform grain size D, equations (4)–(6) can be used to compute the corresponding $Q_{\mathrm{sat}}/Q_{\mathrm{sat}}^0$ value (Figure 2b). Then, using the dependency of the $Q_{\mathrm{sat}}/Q_{\mathrm{sat}}^0$ value on the threshold shear stress in the model (Figure 2c), we can derive the τ_1 value that should be used in the simulations from the mean wind speed in the field [*Narteau et al.*, 2009].

Let us now consider granular mixtures with fine and coarse grains of diameters D_f and D_c, respectively. In the model of sediment transport, mobile and immobile sedimentary states may be decomposed into substates according to specific physical properties, for example, grain size (Figure 2a). In this case, all transitions remain the same but the threshold shear stress is rescaled according to both grain size and flow speed following the procedure described above. Then we have $\tau_1^{\mathrm{f}} < \tau_1^{\mathrm{c}}$, where τ_1^{f} and τ_1^{c} are the threshold shear stress for fine and coarse grains, respectively (Figure 2c). For the sake of simplicity, all sedimentary cells are assumed to be independent from one another and there is no effect of the composition of the bed on the threshold shear stress (i.e., the $\tau_1^{\mathrm{f,c}}$ values are constant in space and time).

To simulate avalanches in granular mixtures we use the model of *Makse et al.* [1997], which considers two repose angles for each grain size and a two-phase dynamic. Considering smaller repose angles for coarse grains, this model is known to generate stratification and segregation. As described in Text S1 of the supporting information, this is also the case in our model.

3. Development of Dunes and Vertical Sorting in Granular Mixtures

Simulations are conducted under a steady unidirectional flow in a wind tunnel with periodic horizontal boundary conditions (Figure S3 in the supporting information). The initial condition is a flat bed composed of a mixture of two populations of fine and coarse grains (Figures 3a and 3b at $t = 0$). The thickness of the mixed sediment is high enough with respect to the depth of the flow to ensure that dunes converge to a steady state before reaching the base of the cellular space [*Gao et al.*, 2015a].

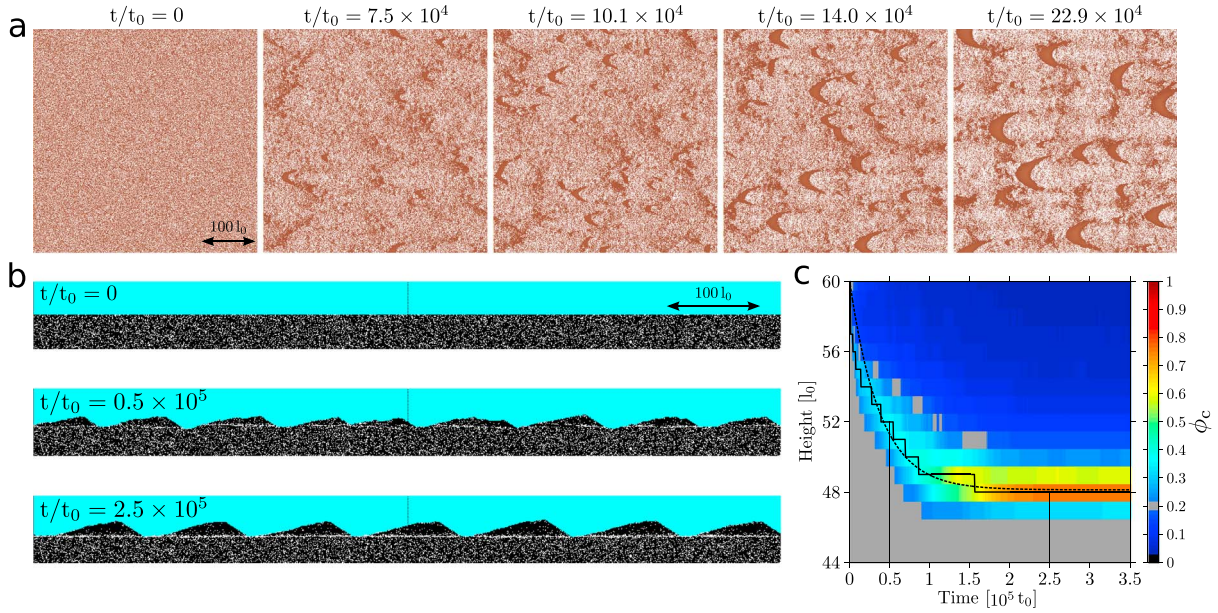


Figure 3. Development of dune fields and dynamical armoring in the model. (a) Top views of the dune field for Q^c_{sat}/Q^f_{sat} =1/32 and ϕ_c =0.3. (b) Vertical sections of the dune field for Q^c_{sat}/Q^f_{sat} =1/2 and ϕ_c =0.2. Coarse sedimentary cells are shown in white. (c) Evolution of the proportion of coarse grains with respect to depth for the simulation shown in Figure 3b. The black line shows the depth with the highest proportion of coarse grains. The dashed line is the best exponential fit with a characteristic rate of $2.6 \times 10^{-5}\ t_0^{-1}$.

We explore a two-dimensional parameter space by varying ϕ_c, the initial proportion of coarse grains within the bed, and Q^c_{sat}/Q^f_{sat}, the ratio between the saturated fluxes for coarse and fine sediment. From equations (4) and (6), we have

$$\frac{D_c}{D_f} = \frac{Q^0_{sat} - Q^c_{sat}}{Q^0_{sat} - Q^f_{sat}}. \tag{7}$$

Under transport limited conditions (i.e., $Q^f_{sat} > Q^c_{sat} > 0$), the grain size ratio D_c/D_f can therefore be derived from the sand flux ratio Q^c_{sat}/Q^f_{sat} (see Figures 2b and Figures S4 and S5 in the supporting information). Simulations are run for $\phi_c = \{0.1, 0.2, 0.3, 0.4, 0.5, 0.6, 0.7, 0.8, 0.9\}$ and $Q^c_{sat}/Q^f_{sat} = \{2/3, 1/2, 1/4, 1/8, 1/16, 1/32\}$. Applied to aeolian transport and considering a fine grain size D_f = 168 µm and a wind speed u=20 m/s at a height z of 10 m, these flux ratios correspond to $D_c/D_f = \{8.4, 12.1, 17.7, 20.4, 21.8, 22.5\}$ (see Tables S1 and S2 in the supporting information for other scalings in various geophysical environments).

For two different initial compositions of the bed, Figures 3a and 3b show the formation of a barchan and a transverse dune fields in the model, respectively [*Werner*, 1995]. In both cases, generic behaviors may be observed during the development of bed forms. Over short times, fine grains preferentially move and start to form clusters from which small dune features develop. Coarse grains also participate in transport but, as they have a larger entrainment threshold, they are less likely to be incorporated into these incipient bed forms and they tend to concentrate in the lower parts of the bed. When slip faces appear on the lee face of dunes, avalanches also concentrate coarse grains that reach the crest in topographic lows. As a result of these mechanisms of size segregation (i.e., selective transport and avalanches), a coarse surface layer develops and rapidly protects the underlying bed from wind erosion. This coarse layer flattens as the dunes propagate because the reduction of wind speed results in the winnowing of fines at the dune toes or in the interdune areas (i.e., areas where $\tau^c_1 > \tau_s > \tau^f_1$, especially dune troughs). Finally, dunes migrate on a flat armor layer as observed in the field (Figure 1).

Figure 3c shows the evolution of the proportion of coarse grains with respect to depth. The exponential relaxation to a steady state suggests that armoring and vertical grain size sorting are part of the same dynamic process, which occur at a constant rate. It involves mixing of a few layers of sedimentary cells such that the proportion of coarse grains just below the armor may also be higher than the proportion within the initial bed.

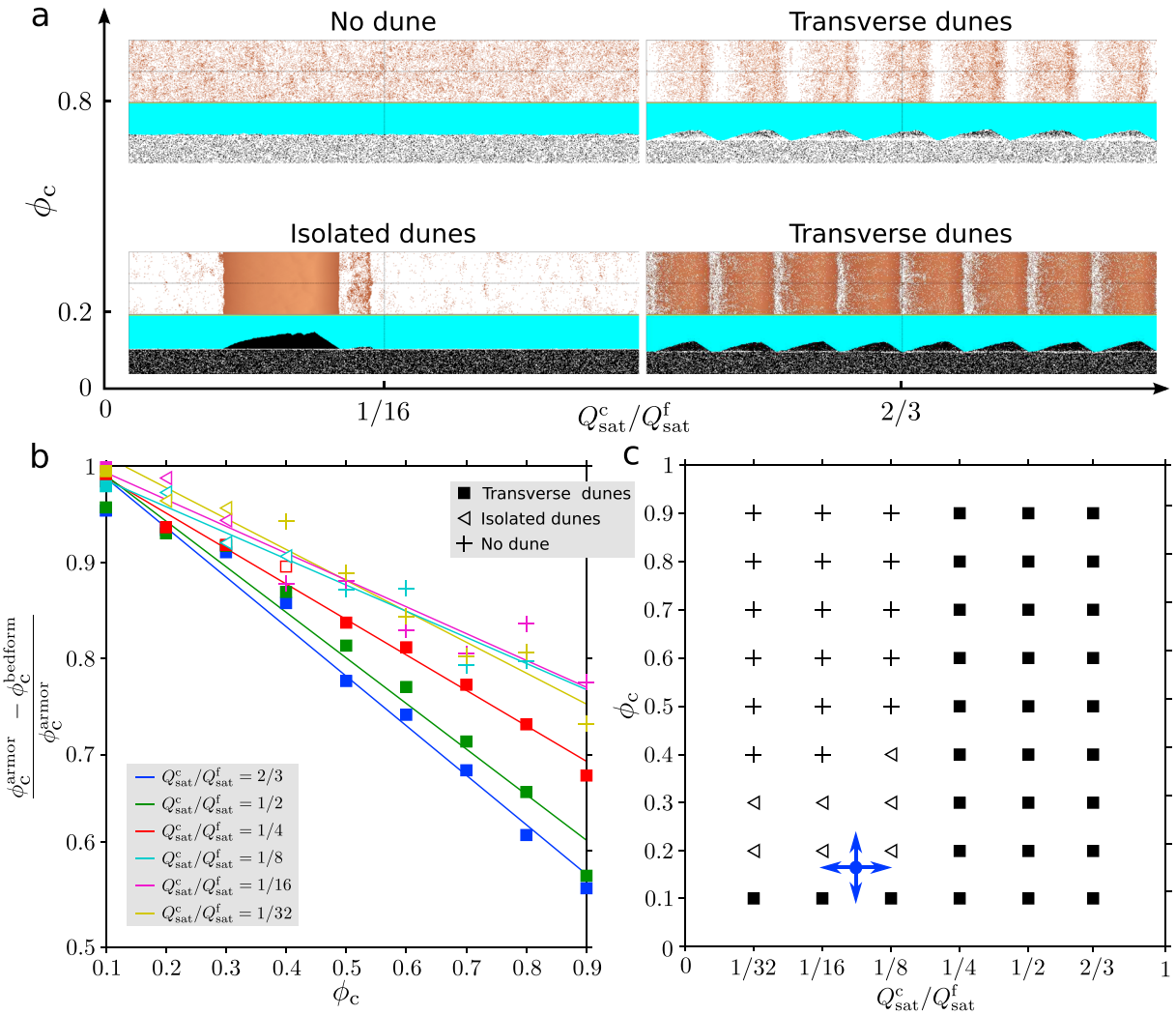


Figure 4. Characterization of steady state dune fields in granular mixtures. (a) Classification of dune types in the model. (b) The degree of sediment sorting $(1 - \phi_c^{bedform}/\phi_c^{armor})$ with respect to the initial proportion of coarse grains ϕ_c for different saturated sand flux ratios Q^c_{sat}/Q^f_{sat}. (c) Phase diagram of dune type in the $\{\phi_c, Q^c_{sat}/Q^f_{sat}\}$ parameter space. The blue dot corresponds to the field example shown in Figure 1 using $D_f = 180\,\mu m$, $D_c/D_f = 20$ and $u = 20$ m/s.

3.1. Characterization of Steady State Dune Fields in Granular Mixtures

As shown in Figure 4, we identify three classes of steady state dune fields in the $\{\phi_c, Q^c_{sat}/Q^f_{sat}\}$ parameter-space (see also Figure S6 in the supporting information):

1. Periodic transverse dunes are observed for high transport ratio (small grain size ratio) or for a small proportion of coarse grain ($\phi_c \leq 0.1$). At the surface of these regular dunes, the proportion of coarse grains decreases with height and it is the highest in the troughs where a mobile pavement is observed (see Figure S7 in the supporting information). As this armor layer develops, the trough areas reach a constant elevation across the entire dune field.
2. For intermediate values of the proportion of coarse grains ($0.1 < \phi_c < 0.4$) and low transport ratio (high grain size ratio), isolated dunes composed of fine grains migrate on a flat and static armor layer of coarse grains.
3. When the transport ratio is low (high grain size ratio) and the proportion of coarse grain is high, there is no dune. Instead, sudden changes in bed roughness may be related to spatial variation of the bed composition and transient patches of fine grains.

Figure 4b shows that the proportion of coarse grains within the armor layer is at least twice the proportion within the overlying dunes (i.e., $\phi_c^{armor} \geq 2\phi_c^{bedform}$). Then, vertical grain size sorting and dynamical armoring

control sand availability and the subsequent dune type. When the initial proportion of coarse grains is high, it leads to a transition from transverse dunes to no dune for a decreasing transport ratio (i.e., an increasing grain size ratio). For a smaller proportion of coarse grains, individual patches of fines grain may produce isolated dunes, and a transition from transverse to barchan dune fields may be observed for a decreasing transport ratio (i.e., an increasing grain size ratio).

4. Concluding Remarks

It is well established that aeolian transport is efficient in sorting grainsize, but contrary to subaqueous cases [*Blom et al.*, 2003; *Murray and Thieler*, 2004; *Coco et al.*, 2007a; *Blondeaux*, 2012; *Bacchi et al.*, 2014], there is still no numerical study dedicated to such a dynamic process in relation with dune growth. The real-space cellular automaton dune model appears to be particularly adapted to this purpose because the state of elementary cells can be used to distinguish between different grain sizes (Figure 2a). As described in *Narteau et al.* [2009], these elementary cells have a dimension which is a few orders of magnitude larger than individual grains, such that the rules of the model integrate over smaller length scales the effect of particle interactions on the overall transport rate. Thus, we concentrate on patterns which result only from the dune instability and we can investigate the dynamics of a significant portion of a dune field as well as the behaviors of giant dunes [*Zhang et al.*, 2012; *Gao et al.*, 2015b].

Our numerical dune model complements the model of *Anderson and Bunas* [1993], which is only dedicated to the development of aeolian ripples. In the current study, dunes appear to segregate toward fine crests while at the ripple scale bed forms self-organize into coarse crests. In part this is because ripples have no avalanche faces, their lee slope inclination never exceeds the angle of repose, which in turn disallows the return of coarse grains to the base of the bed forms. In addition, ripple dynamics is mainly controlled by the impact of saltating grains; coarse grains are less likely to be set in motion and, as their hop length determines the ripple wavelength, they get stuck on the crest, while the fine grains can land in the troughs. Comparing the numerical results of ripple and dune models, differences in segregation patterns show the importance of addressing each type of bed form with the relevant set of physical quantities: entrainment threshold, the saturated flux and the saturation length and time scales for dunes [see a review in *Durán et al.*, 2011]; saltation length and wind speed for ripples [*Anderson*, 1988; *Anderson and Bunas*, 1993; *Durán et al.*, 2014].

There is a spectrum of grain sizes that characterizes the coarse-grained surfaces in arid deserts [*Laity*, 2011]. In many cases, desert pavements consist of very coarse sediment that are beyond the realm of wind transport [*Haff and Werner*, 1996]. These are interpreted as lags of wind deflated fluvial-sourced sediment. In this case, dust and fine sediment may infiltrate downward and the surface veneer may be raised [*Wells et al.*, 1985]. Using a numerical dune model, we concentrate here on grain sizes within the range of what can be moved by the wind on a flat surface. Exploring the parameter space of granular binary mixtures, our primary focus is to describe steady state dune fields from a set of well-established initial and boundary conditions. This is the first step in the modeling of geomorphic processes in systems with a wide range of grain sizes, which are intrinsically more complicated. This is also why we concentrate only on behaviors which do not depend on sediment supply, the initial amount of sediment on the nonerodible basement and the cumulative transport [*Ewing and Kocurek*, 2010; *Eastwood et al.*, 2011]. However, our numerical approach is now ready to be used with more realistic boundary conditions to explore downwind fining [*Jerolmack et al.*, 2006] as well as desert pavements and their effect on sediment transport.

In our simulations, we consider that there is no influence of the bed texture on the entrainment of individual grains and that differential transport and avalanches are the only sources of size segregation [*Coco et al.*, 2007a, 2007b]. We show that vertical sorting always occurs leading to the formation of an armor layer on the top of which dunes essentially composed of fine material migrate. Overall, this sorting mechanism controls sand availability and the subsequent dune types. Using granulometric data and wind speed in the Kumtagh Desert [*Dong et al.*, 2008; *Liu et al.*, 2014], we can find where the dune field shown in Figure 1 lies within the parameter space explored by the numerical simulations (blue dot in Figure 4c). In practice, $\phi_c = 0.17 \pm 0.08$ and $Q^c_{sat}/Q^f_{sat} = 1/12.4$ using $D_f = 180\,\mu m$, $D_c/D_f = 20$ and $u = 20\,m/s$ (see the bimodal distribution in Figure 1e). As observed in the field, the model predicts isolated dunes that propagate on a coarse bed layer (see Figure 1 and Figures S8 and S9 in the supporting information).

Using only grain sizes that can be set in motion by the wind, our model achieves segregation and hence effectively decouples the dunes from the bed. In reality, other mechanisms and problem setups/initial conditions

can serve the same purpose and coexist with the dynamical size-segregation process investigated here. This is the case in our field example where we should account for specific boundary conditions, the alluvial origin of the subsurface deposit and the presence of coarse grains never involved in the transport system. In the framework of the model, gravels are just passive agents and a natural end-member for $Q_{sat}^{c}/Q_{sat}^{f} \rightarrow 0$ (see Figure S10 of the supporting information how isolated barchans develop from a bed composed at 30% of gravels). From the original deposit containing these coarse grains, the surface has been fully reworked by the wind and the observed armor layer is the result of aeolian selective transport, which is still active nowadays. There are no river channels or signs of hydraulic reworking in the dune field. Instead, the surface is permanently evolving under wind action (see Figure S9 of the supporting information) and there are clear signs of abrasion by sand blasting, which indicate that the bombarding of the surface by airborne particles is the dominant process (see Figure S11 of the supporting information). The presence of yardangs just a few kilometers southeast confirms such a hypothesis. Finally, the observed barchans in the field may not be directly the result of the segregation of fine particles from the subsurface material shown in Figure 1f, simply because the corresponding dunes may have already migrated downwind, replaced by others due to the continuous supply of sand from upwind (see Figure S12 of the supporting information).

Sand availability is a critical control parameter in multidirectional wind regimes where transitions in dune shape and orientation are ubiquitous [*Gao et al.*, 2015b]. This is particularly true when considering that dunes may either grow by lateral accretion under conditions of high sand availability [*Rubin and Hunter*, 1987; *Ping et al.*, 2014] or by extension in zones of limited sand supply [*Courrech du Pont et al.*, 2014; *Lucas et al.*, 2015]. The present study explains how dunes may align in different directions according to the initial configuration of the bed in major depositional centers. Then, we conclude that despite the natural complexities in terrestrial sand seas, the observed dune types and orientations may help in characterizing the grain size distribution over space and time. All this information is also critical on other planetary bodies, such as Mars and Titan, where the sediment properties and the origin of the dune fields are still under investigation [*Lucas et al.*, 2014; *Charnay et al.*, 2015].

Acknowledgments
Authors thank Brad Murray, Bob Anderson, and an anonymous reviewer for their constructive remarks. We also thank Sylvain Courrech du Pont for his comments on the manuscript. We are grateful to Zhibao Dong and Ping Lv for their assistance in the Kumtagh Desert. The data present in this paper are the result of numerical simulations using ReSCAL, the Real-Space Cellular Automaton Laboratory. ReSCAL is a free software under the GNU general public licence. The source codes can be downloaded from http://www.ipgp.fr/rescal. We acknowledge financial support from the UnivEarthS LabEx program of Sorbonne Paris Cité (ANR-10-LABX-0023 and ANR-11-IDEX-0005-02) and the French National Research Agency (ANR-09-RISK-004/GESTRANS and ANR-12-BS05-001-03/EXO-DUNES). Figure 1a is courtesy of Google Earth. Data and picture shown in Figures 1e and 1f are provided by Guangqiang Qian.

References

Anderson, R. S. (1988), The pattern of grainfall deposition in the lee of aeolian dunes, *Sedimentology*, *35*(2), 175–188, doi:10.1111/j.1365-3091.1988.tb00943.x.
Anderson, R. S., and K. L. Bunas (1993), Grain size segregation and stratigraphy in aeolian ripples modelled with a cellular automaton, *Nature*, *365*, 740–743, doi:10.1038/365740a0.
Andreotti, B., P. Claudin, and O. Pouliquen (2010), Measurements of the aeolian sand transport saturation length, *Geomorphology*, *123*(3), 343–348, doi:10.1016/j.geomorph.2010.08.002.
Bacchi, V., A. Recking, N. Eckert, P. Frey, G. Piton, and M. Naaim (2014), The effects of kinetic sorting on sediment mobility on steep slopes, *Earth Surf. Process. Landforms*, *39*(8), 1075–1086, doi:10.1002/esp.3564.
Blom, A., J. S. Ribberink, and H. J. de Vriend (2003), Vertical sorting in bed forms: Flume experiments with a natural and a trimodal sediment mixture, *Water Resour. Res.*, *39*(2), 1025, doi:10.1029/2001WR001088.
Blom, A., J. S. Ribberink, and G. Parker (2008), Vertical sorting and the morphodynamics of bed form-dominated rivers: A sorting evolution model, *113*, F01019, doi:10.1029/2006JF000618.
Blondeaux, P. (2012), Sediment mixtures, coastal bedforms and grain sorting phenomena: An overview of the theoretical analyses, *Adv. Water Resour.*, *48*, 113–124, doi:10.1016/j.advwatres.2012.02.004.
Charnay, B., E. Barth, S. Rafkin, C. Narteau, S. Lebonnois, S. Rodriguez, S. Courrech du Pont, and A. Lucas (2015), Methane storms as a driver of Titan's dune orientation, *Nat. Geosci.*, *8*, 362–368, doi:10.1038/ngeo2406.
Cizeau, P., H. A. Makse, and H. E. Stanley (1999), Mechanisms of granular spontaneous stratification and segregation in two-dimensional silos, *Phys. Rev. E*, *59*, 4408–4421, doi:10.1103/PhysRevE.59.4408.
Coco, G., A. B. Murray, and M. O. Green (2007a), Sorted bed forms as self-organized patterns: 1. Model development, *J. Geophys. Res.*, *112*, F03015, doi:10.1029/2006JF000665.
Coco, G., A. B. Murray, M. O. Green, E. R. Thieler, and T. Hume (2007b), Sorted bed forms as self-organized patterns: 2. Complex forcing scenarios, *J. Geophys. Res.*, *112*, F03016, doi:10.1029/2006JF000666.
Courrech du Pont, S., C. Narteau, and X. Gao (2014), Two modes for dune orientation, *Geology*, *42*(9), 743–746, doi:10.1130/G35657.1.
Dietrich, W. E., J. W. Kirchner, H. Ikeda, and F. Iseya (1989), Sediment supply and the development of the coarse surface layer in gravel-bedded rivers, *Nature*, *340*(6230), 215–217.
Dong, Z., J. Qu, X. Wang, G. Qian, W. Luo, and Z. Wei (2008), Pseudo-feathery dunes in the Kumtagh Desert, *Geomorphology*, *100*(3), 328–334, doi:10.1016/j.geomorph.2008.01.004.
Durán, O., P. Claudin, and B. Andreotti (2011), On aeolian transport: Grain-scale interactions, dynamical mechanisms and scaling laws, *Aeolian Res.*, *3*(3), 243–270, doi:10.1016/j.aeolia.2011.07.006.
Durán, O., P. Claudin, and B. Andreotti (2014), Direct numerical simulations of aeolian sand ripples, *Proc. Natl. Acad. Sci. U.S.A.*, *111*(44), 15,665–15,668, doi:10.1073/pnas.1413058111.
Eastwood, E., J. Nield, A. Baas, and G. Kocurek (2011), Modelling controls on aeolian dune-field pattern evolution, *Sedimentology*, *58*(6), 1391–1406, doi:10.1111/j.1365-3091.2010.01216.x.
Ewing, R. C., and G. A. Kocurek (2010), Aeolian dune interactions and dune-field pattern formation: White sands dune field, New Mexico, *Sedimentology*, *57*(5), 1199–1219, doi:10.1111/j.1365-3091.2009.01143.x.
Frey, P., and M. Church (2009), How river beds move, *Science*, *325*(5947), 1509–1510, doi:10.1126/science.1178516.

Gao, X., D. Zhang, O. Rozier, and C. Narteau (2014), Transport capacity and saturation mechanism in a real-space cellular automaton dune model, *Adv. Geosci.*, *37*, 47–55, doi:10.5194/adgeo-37-47-2014.
Gao, X., C. Narteau, and O. Rozier (2015a), Development and steady states of transverse dunes: A numerical analysis of dune pattern coarsening and giant dunes, *J. Geophys. Res. Earth Surf.*, *120*, 2200–2219, doi:10.1002/2015JF003549.
Gao, X., C. Narteau, O. Rozier, and S. Courrech du Pont (2015b), Phase diagrams of dune shape and orientation depending on sand availability, *Sci. Rep.*, *5*, 14677, doi:10.1038/srep14677.
Haff, P. K., and B. T. Werner (1996), Dynamical processes on desert pavements and the healing of surficial disturbances, *Quat. Res.*, *45*(1), 38–46.
Houssais, M., and E. Lajeunesse (2012), Bedload transport of a bimodal sediment bed, *J. Geophys. Res.*, *117*, F04015, doi:10.1029/2012JF002490.
Iversen, J. D., and K. R. Rasmussen (1999), The effect of wind speed and bed slope on sand transport, *Sedimentology*, *46*(4), 723–731, doi:10.1046/j.1365-3091.1999.00245.x.
Jerolmack, D. J., D. Mohrig, J. P. Grotzinger, D. A. Fike, and W. A. Watters (2006), Spatial grain size sorting in eolian ripples and estimation of wind conditions on planetary surfaces: Application to Meridiani Planum, Mars, *J. Geophys. Res.*, *111*, E12S02, doi:10.1029/2005JE002544.
Laity, J. E. (2011), Pavements and stone mantles, in *Arid Zone Geomorphology: Process, Form and Change in Drylands, Third Edition*, edited by D. S. G. Thomas, pp. 181–207, Wiley Online Library, U. K.
Lancaster, N. (1986), Grain-size characteristics of linear dunes in the southwestern Kalahari, *J. Sediment. Petrol.*, *56*(3), 395–400.
Liu, B., J. Qu, D. Ning, Y. Gao, R. Zu, and Z. An (2014), Grain-size study of aeolian sediments found east of Kumtagh Desert, *Aeolian Res.*, *13*, 1–6, doi:10.1016/j.aeolia.2014.01.001.
Lucas, A., et al. (2014), Growth mechanisms and dune orientation on Titan, *Geophys. Res. Lett.*, *41*(17), 6093–6100, doi:10.1002/2014GL060971.
Lucas, A., C. Narteau, S. Rodriguez, O. Rozier, Y. Callot, A. Garcia, and S. Courrech du Pont (2015), Sediment flux from the morphodynamics of elongating linear dunes, *Geology*, *43*(11), 1027–1030, doi:10.1130/G37101.1.
Makse, H. A., S. Havlin, P. R. King, and H. E. Stanley (1997), Spontaneouos stratification in granular mixtures, *Nature*, *386*, 379–382.
Murray, A. B., and E. R. Thieler (2004), A new hypothesis and exploratory model for the formation of large-scale inner-shelf sediment sorting and "rippled scour depressions", *Cont. Shelf Res.*, *24*(3), 295–315, doi:10.1016/j.csr.2003.11.001.
Narteau, C., D. Zhang, O. Rozier, and P. Claudin (2009), Setting the length and time scales of a cellular automaton dune model from the analysis of superimposed bed forms, *J. Geophys. Res.*, *114*, F03006, doi:10.1029/2008JF001127.
Parker, G., and P. Klingeman (1982), On why gravel bed streams are paved, *Water Resour. Res.*, *18*(5), 1409–1423, doi:10.1029/WR018i005p01409.
Parker, G., C. Paola, and S. Leclair (2000), Probabilistic Exner sediment continuity equation for mixtures with no active layer, *J. Hydraul. Eng.*, *126*(11), 818–826.
Ping, L., C. Narteau, Z. Dong, Z. Zhang, and S. Courrech du Pont (2014), Emergence of oblique dunes in a landscape-scale experiment, *Nat. Geosci.*, *7*, 99–103, doi:10.1038/ngeo2047.
Rozier, O., and C. Narteau (2014), A real-space cellular automaton laboratory, *Earth Surf. Process. Landforms*, *39*, 98–109, doi:10.1002/esp.3479.
Rubin, D. M., and R. E. Hunter (1987), Bedform alignment in directionally varying flows, *Science*, *237*, 276–278.
Sherman, D. J., and B. Li (2012), Predicting aeolian sand transport rates: A reevaluation of models, *Aeolian Res.*, *3*(4), 371–378, doi:10.1016/j.aeolia.2011.06.002.
Staron, L., and J. C. Phillips (2014), Segregation time-scale in bi-disperse granular flows, *Phys. Fluids*, *26*, 033302, doi:10.1063/1.4867253.
Thomas, D. S. G. (2011), *Arid Zone Geomorphology: Process, Form and Change in Drylands, Third Edition*, 624 pp., John Wiley, U. K.
Wasson, R. J., and R. Hyde (1983), Factors determining desert dune types, *Nature*, *304*, 337–339, doi:10.1038/304337a0.
Wells, S. G., J. C. Dohrenwend, L. D. McFadden, B. D. Turrin, and K. D. Mahrer (1985), Late cenozoic landscape evolution on lava flow surfaces of the Cima volcanic field, Mojave Desert, California, *Geol. Soc. Amer. Bull.*, *96*(12), 1518–1529.
Werner, B. T. (1995), Eolian dunes: Computer simulations and attractor interpretation, *Geology*, *23*(12), 1107–1110.
Wilcock, P. R. (2001), Toward a practical method for estimating sediment-transport rates in gravel-bed rivers, *Earth Surf. Process. Landforms*, *26*(13), 1395–1408, doi:10.1002/esp.301.
Wilcock, P. R., and J. B. Southard (1989), Bed load transport of mixed size sediment: Fractional transport rates, bed forms, and the development of a coarse bed surface layer, *Water Resour. Res.*, *25*(7), 1629–1641, doi:10.1029/WR025i007p01629.
Zhang, D., C. Narteau, O. Rozier, and S. Courrech du Pont (2012), Morphology and dynamics of star dunes from numerical modelling, *Nat. Geosci.*, *5*, 463–467, doi:10.1038/ngeo1503.
Zhang, D., X. Yang, O. Rozier, and C. Narteau (2014), Mean sediment residence time in barchan dunes, *J. Geophys. Res.*, *119*, 451–463, doi:10.1002/2013JF002833.